MECH513 Project Part 1

Frequency Domain System Identification and Uncertainty Modeling of Coolant Pump for McGill Formula Electric 2025 Car

Lucas Bessai, 261050265
Aidan Kimberly, 261004905
Department of Mechanical Engineering, McGill University
817 Sherbrooke Street West, Montreal, QC, H3A 0C3

November 11, 2025

1 Introduction

The overall goal of this project is to design a feedback controller for a pump used to cool the motors of a Formula-E vehicle. The pump must regulate coolant flow efficiently to maintain target motor temperatures while minimizing electrical energy drawn from the low-voltage battery. Achieving this trade-off requires an accurate dynamic model of how pump voltage input affects flow output under realistic operating conditions. Since this relationship is not analytically known and varies with hardware, system identification is used to infer a mathematical model directly from experimental input–output data. In turn, uncertainty characterization quantifies how much the identified model can deviate from the true plant. This ensures that the controller designed around the nominal model will remain stable and perform acceptably even if the physical pump behaves slightly differently—an essential requirement for robustness in safety-critical systems.

We identify a continuous-time nominal plant $P_0(s)$ for the pump (input: voltage u, output: flow y) from chirp experiments and then characterize model uncertainty for robust control. The workflow is: (i) compute a frequency response using estimates of cross/auto spectral densities with a Hann window; (ii) prune unreliable frequency points using coherence and Nyquist criteria; (iii) fit low-order rational transfer functions to each dataset to form off-nominal plants $P_k(s)$ using median coefficients; and (v) fit a multiplicative uncertainty weight $W_2(s)$ that upper-bounds the residuals. The objective is a conservative, controller-ready model set rather than a maximally accurate plant.

2 Nominal Model Identification

2.1 Frequency-domain estimation from time data

Given time data $u(t_i)$ and $y(t_i)$ sampled with period T_s, the columns were separated and the cross power spectral desity was computed using the scipy signal library. Under the hood the time data is multiplied by a Hanning window $w[n]$. The Hanning window tappers on both ends to avoid discontinuity and spectral leakage. This tappering of the signal reduces resolution of the active frequencies in the signal but in the end gives a better estimate of the frequency response of the system. For each segment of he signal, a one-sided discrete Fourier transforms is computed, and Welch estimates of the power spectral densities were formed as

$$\Phi_{uu}(\omega) = \mathrm{E}[U(\omega)U^*(\omega)], \qquad \Phi_{yy}(\omega) = \mathrm{E}[Y(\omega)Y^*(\omega)], \qquad \Phi_{uy}(\omega) = \mathrm{E}[U(\omega)Y^*(\omega)]. \tag{1}$$

The discrete frequency response was then obtained as

$$\hat{P}(\mathrm{j}\omega) = \frac{\Phi_{uy}(\omega)}{\Phi_{uu}(\omega)}. \tag{2}$$

In contrast to the raw FFT ratio Y/U which is biased when $|U|$ is very small. Coherence,

$$\gamma^2(\omega) = \frac{|\Phi_{uy}(\omega)|^2}{\Phi_{uu}(\omega)\,\Phi_{yy}(\omega)}, \tag{3}$$

is a measure of how linear the relationship between u and y is at each frequency, ω. Thus, it was used to remove unreliable frequency points. Frequencies with $\gamma^2(\omega) < 0.8$, frequencies above $0.9\,\omega_N$ (Nyquist limit), and those with small Φ_{uu} were discarded. Only the high-frequency region near the Nyquist limit displayed low coherence, confirming that the dominant nonlinearity originated from sampling noise rather than the pump.

2.2 Parametric fitting of off-nominal plants

Each dataset was fit independently with a continuous-time, rational transfer function of chosen orders (m, n):

$$P(s) = \frac{b_m s^m + b_{m-1} s^{m-1} + \cdots + b_0}{s^n + a_{n-1} s^{n-1} + \cdots + a_0}, \qquad n > m. \tag{4}$$

The model parameters were obtained through a complex least-squares fit to the discrete frequency data:

$$\min_{\theta} \sum_k w_k \left| P(\mathrm{j}\omega_k; \theta) - \hat{P}(\mathrm{j}\omega_k) \right|^2, \tag{5}$$

where w_k weights each frequency according to its coherence. This gives more emphasis to frequencies that display more linearity. Rearranging the transfer function equation gives a linear system in the coefficients:

$$\hat{P}_k[(\mathrm{j}\omega_k)^n + a_{n-1}(\mathrm{j}\omega_k)^{n-1} + \cdots + a_0] = b_m(\mathrm{j}\omega_k)^m + \cdots + b_0, \tag{6}$$

which is solved by splitting the real and imaginary domain and stacking the regressor matrix:

$$\begin{bmatrix} Re(A) \\ Im(A) \end{bmatrix} x = \begin{bmatrix} Re(b) \\ Im(b) \end{bmatrix} \tag{7}$$

The four resulting models from the four input-output data sets $\{P_k(s)\}_{k=1}^4$ represent the off-nominal plants.

2.3 Model order selection

Model quality was evaluated using both time and frequency-domain metrics:

$$\mathrm{VAF} = \left(1 - \frac{\mathrm{var}(y - \hat{y})}{\mathrm{var}(y)}\right) \times 100, \tag{8}$$

$$\mathrm{NMSE}_\omega = \frac{\sum_k w_k |\hat{P}(\mathrm{j}\omega_k) - P(\mathrm{j}\omega_k)|^2}{\sum_k w_k |\hat{P}(\mathrm{j}\omega_k)|^2}. \tag{9}$$

Higher-order numerators often improved these score; however, roll-off occurs near the Nyquist limit where reliable data thin out. A first-order model captured the dominant behavior with fewer assumptions, and—crucially—avoids over-interpreting high-frequency roll-off we did not reliably excite. We therefore chose a first-order model on conservatism grounds. Figure 1 illustrates the stronger fit achieved by higher order models.

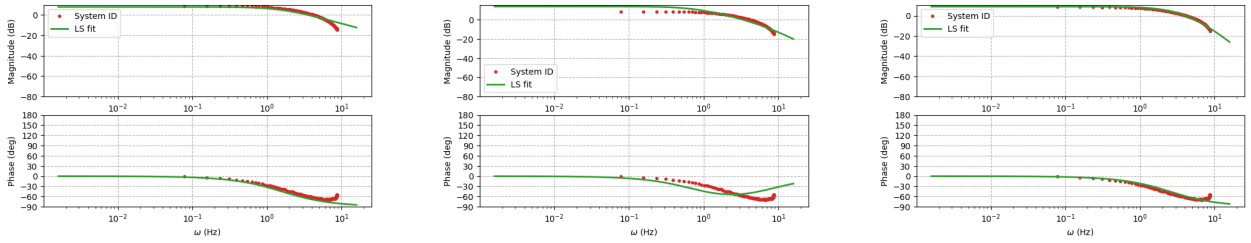

((a)) 1st Order ((b)) 2nd Order ((c)) 3rd Order

Figure 1: Fit of transfer functions of increasing denominator order to discrete frequency response

As shown in Figure 1 the fit becomes increasing tight as order of transfer function increases. This is natural as a more and more complex polynomial will fit to any function eventually. The data in table 1 shows that the first order model was able to adequately capture the dynamics of the system. Specifically, the variance acounted for is suitabley high for all train-test cases.

Table 1: Frequency and time-domain fit metrics across train–test splits (all models fixed at $(m, n) = (1, 1)$).

Train	**Test**	$\mathbf{F}_{\mathrm{MSE}}$	$\mathbf{F}_{\mathrm{NMSE}}$	$\boldsymbol{\sigma}_{\mathbf{max}}$	$\mathbf{rel}\%_{\max}$	$\mathbf{NMSE_t}$	$\mathbf{VAF}\%$
0	0	16.208	0.075	0.480	12.15	0.026	97.39
0	1	28.076	0.277	0.834	20.81	0.218	78.25
0	2	26.020	0.110	0.767	18.16	0.093	90.67
0	3	7.551	0.045	0.377	12.79	0.016	98.37
1	1	3.724	0.037	0.304	10.79	0.022	97.80
1	0	42.403	0.197	0.776	27.98	0.157	84.32
1	2	46.670	0.198	1.027	34.63	0.117	88.30
1	3	27.164	0.162	0.716	34.55	0.154	84.58
2	2	10.579	0.045	0.489	6.02	0.027	97.34
2	0	35.718	0.166	0.712	9.38	0.058	94.16
2	1	41.164	0.406	1.010	13.11	0.057	94.26
2	3	39.786	0.237	0.866	15.28	0.089	91.06
3	3	4.126	0.025	0.279	19.37	0.021	97.90
3	0	20.170	0.094	0.535	27.75	0.049	95.08
3	1	21.897	0.216	0.737	37.64	0.284	71.56
3	2	41.573	0.176	0.969	47.01	0.152	84.84

Notes: All rows use $(m, n) = (1, 1)$, no frequency weights; mask: $\gamma^2 \geq 0.8$, $\Phi_{uu} \geq 0.001 \cdot \mathrm{median}(\Phi_{uu})$, and $f \leq 0.9\, f_{\mathrm{N}}$.

2.4 Nominal model from off-nominals

After obtaining four fitted off-nominal models from the individual datasets, a nominal plant $P_0(s)$ was established to represent the central behavior of the pump. This was achieved by taking the median of each polynomial coefficient across the four transfer functions.

$$b_i^{(0)} = \mathrm{median}(b_{i,1}, b_{i,2}, b_{i,3}, b_{i,4}), \qquad a_i^{(0)} = \mathrm{median}(a_{i,1}, a_{i,2}, a_{i,3}, a_{i,4}), \tag{10}$$

The median is a robust estimator of central tendency that resists the influence of outliers, ensuring that the nominal model represents where most of the identified plants exist rather than being skewed by a single anomalous dataset. In this sense, the median provides a simple and conservative method for centering the model family.

However, this same property is also a limitation because the outlying models will produce larger residuals with respect to the nominal. In the case of a multiplicative uncertainty model, these larger residuals translate to a larger uncertainty bound than would otherwise be necessary. To remedy this, the nominal plant could alternatively be chosen to minimize the residuals of all off-nominal models under a given uncertainty structure—multiplicative being the most suitable choice. This would likely reduce the overall uncertainty bound, which would, in turn, allow for less restrictive gain margins during controller design. Although this optimization approach was considered, the median remains a simple and conservative option that provides a strong starting point for control design. If more aggressive performance targets are required later in the process, this method can be revisited and refined.

As it stands, the median-coefficient nominal characterizes the general behavior of the system identified through the above methodology and fulfills its purpose for the system identification stage. The nominal transfer function is:

$$P_0(s) = \frac{22.67}{s + 10.46} \tag{11}$$

The performance of the nominal plant on all the data sets is shown in figure 2 and 3. When the inputs are normalized the offset error is driven very close to zero.

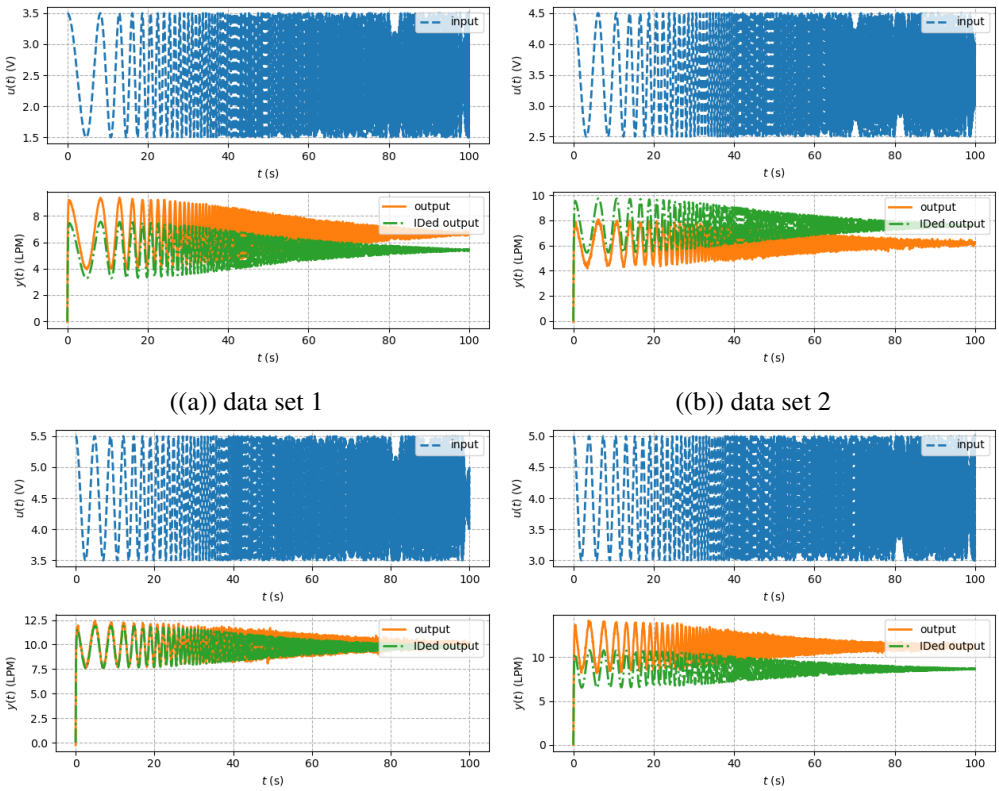

((a)) data set 1

((b)) data set 2

((c)) data set 3

((d)) data set 4

Figure 2: Forced response of nominal plant plotted with measured response

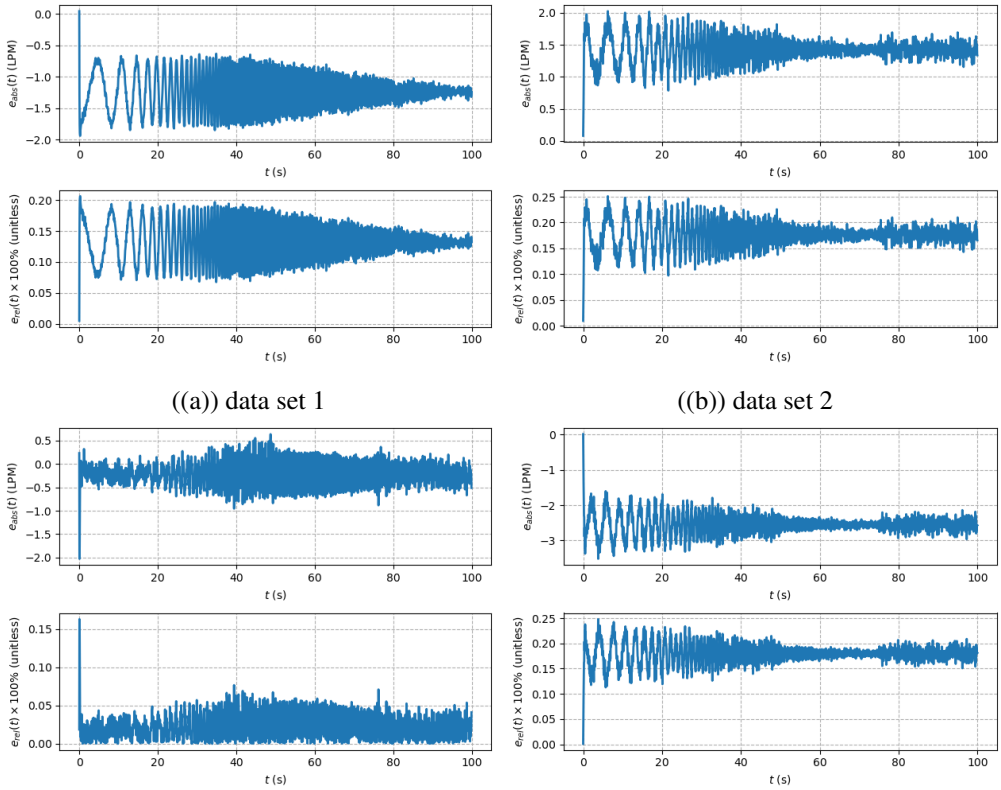

((a)) data set 1 ((b)) data set 2

((c)) data set 3 ((d)) data set 4

Figure 3: Error of nominal plant response and measured response to input chirp signals

”In the end when the application of a model is the design of a controller, then what really matters is the performance achieved by this model-based controller on the true system, and not the intrinsic quality of the model.”(Michel Gevers, 2005) As such, if a first order model with a feedback controller is able to effectively cool the motors for the formula-E car while reducing the battery requirements for constant operation then it has done its job. If more aggressive reduction in weight is required and thus more aggressive gain demands on the controller are required, we will consider a more complex model during the controller design. It is good practice to start simple rather than aim for unnecessary complexity. Figure 4 shows nominal and off-nominal plant bode plots.

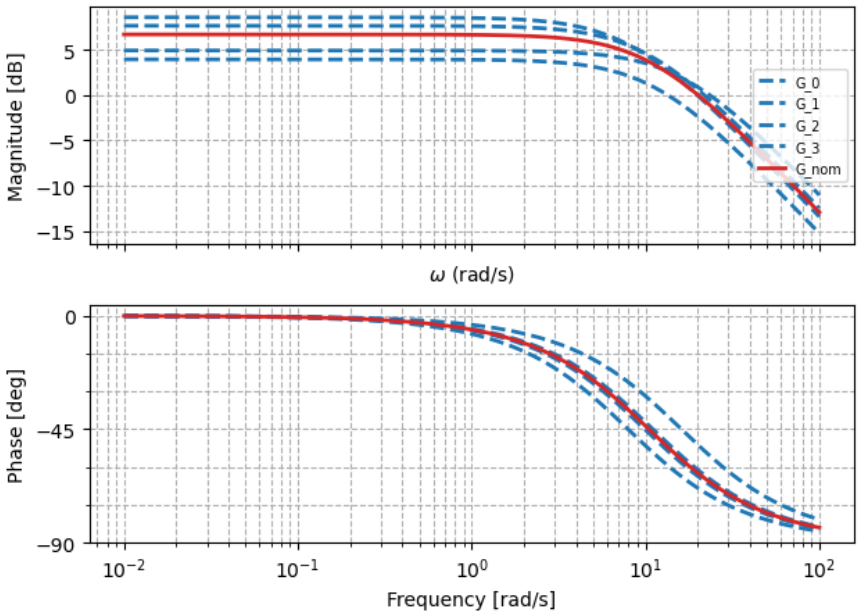

Figure 4: Nominal Plnat plotted with off-nominals

3 Uncertainty Characterization

Four uncertainty structures were tested:

$$\text{Additive:} \quad P_k = P_0 + W_2\Delta_k, \tag{12}$$

$$\text{Multiplicative:} \quad P_k = P_0(1 + \Delta_k W_2), \tag{13}$$

$$\text{Inverse-additive:} \quad P_k^{-1} = P_0^{-1} + W_2\Delta_k, \tag{14}$$

$$\text{Inverse-multiplicative:} \quad P_k^{-1} = P_0^{-1}(1 + \Delta_k W_2), \tag{15}$$

with $\|\Delta_k\|_\infty \leq 1$.

Residual magnitudes were computed as

$$r_k^{\text{add}}(\omega) = |P_k(\mathrm{j}\omega) - P_0(\mathrm{j}\omega)|, \tag{16}$$

$$r_k^{\text{mult}}(\omega) = \left|\frac{P_k(\mathrm{j}\omega) - P_0(\mathrm{j}\omega)}{P_0(\mathrm{j}\omega)}\right|, \tag{17}$$

$$r_k^{\text{ia}}(\omega) = |P_k^{-1}(\mathrm{j}\omega) - P_0^{-1}(\mathrm{j}\omega)|, \tag{18}$$

$$r_k^{\text{im}}(\omega) = \left|\frac{P_k^{-1}(\mathrm{j}\omega) - P_0^{-1}(\mathrm{j}\omega)}{P_0^{-1}(\mathrm{j}\omega)}\right|. \tag{19}$$

The upper envelope $r_{\max}(\omega) = \max_k r_k(\omega)$ was then fit with a low-order, stable, minimum-phase $W_2(s)$ satisfying

$$|W_2(\mathrm{j}\omega)| \geq r_{\max}(\omega) \quad \forall\omega. \tag{20}$$

Figure 5 shows the residual plots for each uncertainty model outlined above.

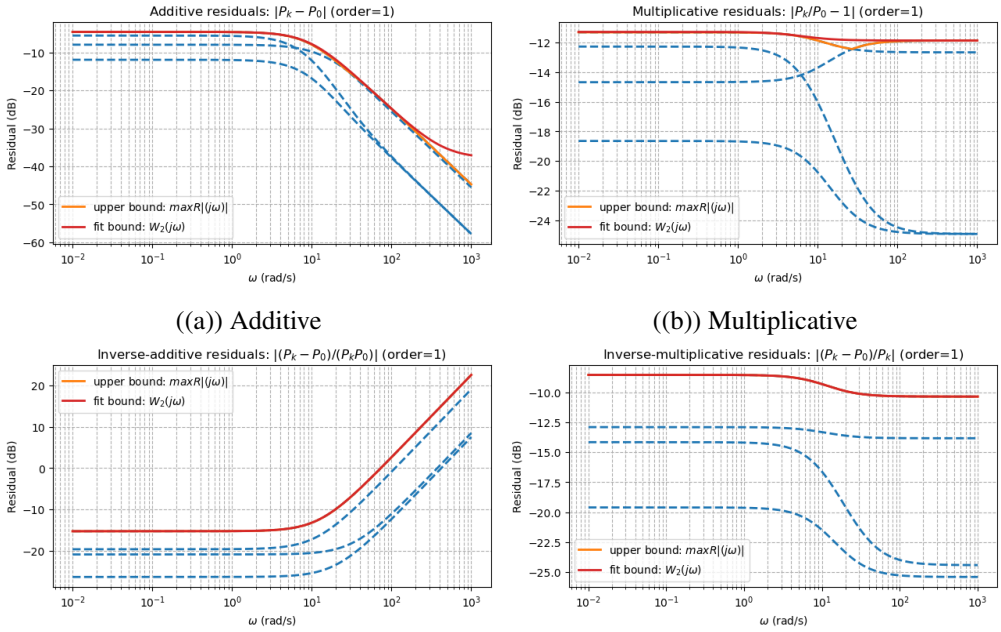

((a)) Additive

((b)) Multiplicative

((c)) Inverse additive

((d)) Inverse multiplicative

Figure 5: Residual plot for each explored uncertainty model. Uncertainty bound W_2 is fit to capture the maximum uncertainty of an off-nominal from the nominal

Additive uncertainty decayed with frequency, making it unsuitable for high-frequency noise representation. Inverse-additive uncertainty increased without bound, leading to poor conditioning. Multiplicative and inverse-multiplicative uncertainties flattened at high frequency, but the multiplicative form produced the smallest bound. Thus, the uncertainty set was defined as

$$\mathcal{P} = \{\, P(s) = P_0(s)[1 + \Delta(s)W_2(s)],\ \|\Delta\|_\infty \leq 1 \,\}. \tag{21}$$

A first-order weight was sufficient:

$$W_2(s) = \kappa \frac{\tau s + 1}{\alpha s + 1} == \frac{0.2551s + 1.675}{s + 6.14}, \tag{22}$$

since higher-order fits offered negligible improvement.

The median-based P_0 can produce slightly larger residuals for outliers, enlarging W_2. This conservatism is acceptable as long as robust stability can be achieved with controller design. The drawback of this is more sluggish performance margins during controller design due to restraints on maximum gains. The code output below quantifies how close the optimal fit weight function is.

```
=== Residual bound tightness ===
Additive              : slack =  7.66 dB |  sup |W2|/max|Rk| =  2.42
Multiplicative        : slack =  0.61 dB |  sup |W2|/max|Rk| =  1.07
Inverse additive      : slack =  0.04 dB |  sup |W2|/max|Rk| =  1.00
Inverse multiplicative: slack =  0.00 dB |  sup |W2|/max|Rk| =  1.00
```

4 Justification for Continued Collaboration

The identification and uncertainty characterization pipeline provides all necessary elements for robust controller design:

- **Reliable frequency-domain data:** Hann-windowed Welch estimates and coherence-based filtering produced high-SNR FRFs with minimal spectral leakage.
- **Conservative, stable nominal:** The first-order median-coefficient model captures dominant pump dynamics and avoids overfitting.
- **Physically consistent uncertainty:** A low-order multiplicative weight $W_2(s)$ bounds the observed model dispersion, aligning with standard robust control formulations.
- **Scalable refinement:** If future performance goals demand tighter margins, P_0 can be re-centered or W_2 reshaped with minimal disruption.

Ultimately, success is measured by closed-loop performance rather than raw identification accuracy. The present P_0, W_2 pair constitutes a sound foundation for robust loop-shaping of the pump-control system, ensuring safe initial gains while leaving room for performance iteration.